Fluorescence Correlation Microscopy of Cells in the Presence of Autofluorescence

Roland Brock, Mark A. Hink, and Thomas M. Jovin
Department of Molecular Biology, Max Planck Institute of Biophysical Chemistry, D-37077 Göttingen, Germany

ABSTRACT Fluorescence correlation microscopy (FCM), the combination of fluorescence correlation spectroscopy (FCS) and digital microscopy (Brock and Jovin, 1998. *Cell. Mol. Biol.* 44:847–856), has been implemented for measuring molecular diffusion and association in living cells with explicit consideration of autocorrelations arising from autofluorescence. Autofluorescence excited at 532 nm colocalizes with mitochondria, has flavin-like spectral characteristics, exhibits relaxation times characteristic for the diffusion of high-molecular-weight proteins, and depends on the incubation conditions of the cells. These time- and location-dependent properties preclude the assignment of universal background parameters. The lower limit for detection of microinjected dextran molecules labeled with the carboxymethylindocyanine dye Cy3 was a few thousand molecules per cell, and the diffusion constant of 1.7×10^{-7} cm^2/s agreed well with values measured with other methods. Based on the fluorescence signal per molecule (*fpm*) and the molecule number derived from autocorrelation analysis, a new method is devised to define intracellular association states. We conclude that FCM is a powerful, noninvasive method for probing molecular interactions in femtoliter volume elements within defined subcellular locations in living cells.

INTRODUCTION

Fluorescence correlation spectroscopy (FCS; Thompson, 1991; Maiti et al., 1997) was developed as a method for measuring molecular diffusibilities and reaction kinetics (Madge et al., 1972, 1974; Elson and Madge, 1974). Diffusion constants and the absolute numbers of fluorescent molecules within a minute observation volume can be derived from fluctuations of the system about equilibrium. These fluctuations are analyzed by forming the autocorrelation function of the fluorescence signal detected with high temporal resolution. Integration of confocal detection optics (Qian and Elson, 1991; Rigler et al., 1993) has led to an increase of the signal-to-noise ratio (SNR), thereby providing the possibility of restricting the measurement to femtoliter volume elements within heterogeneous samples. FCS has been applied to determinations of diffusion in solutions (Madge et al., 1974; Qian et al., 1992) and membranes (Fahey et al., 1977), molecular aggregation (Palmer and Thompson, 1987; Qian and Elson, 1990; Berland et al., 1996), and photophysical processes such as photobleaching and singlet-triplet transitions of fluorophores (Widengren et al., 1994). The technique is gaining considerable acceptance as a sensitive diagnostic tool, as in the analysis of receptor-ligand interactions with solubilized receptors (Rauer et al., 1996) and the hybridization of oligonucleotides to fluorescently labeled target sequences (Oehlenschläger et al., 1996; Walter et al., 1996; Maiti et al., 1997). The recent introduction of dual-color fluorescence cross-correlation in FCS provides the means for probing interactions between molecules bearing different and distinct fluorescent labels (Schwille et al., 1997b). In most of these cited studies the confocal detection principle was used to reduce background and increase detection sensitivity to the single-molecule level. However, few investigators have considered a further consequence of the confocal configuration, namely the capability of analyzing diffusion in heterogeneous multicomponent systems with submicron resolution (Qian et al., 1992; Berland et al., 1995).

We have introduced FCM as a combination of FCS with high-sensitivity imaging, life cell microscopy, fluorescence spectroscopy, micromanipulation, and high precision positioning on one instrumental platform. In this way it is possible to benefit fully from the analytical potential of FCS for investigating molecular processes at the subcellular level (Brock and Jovin, 1998). Inasmuch as the probe volume in a confocal FCM is three orders of magnitude smaller than the typical cellular volume of a few picoliters, molecular association and diffusion can be investigated in specific subcellular compartments. FCS in cuvette measurements with purified molecules achieves a sensitivity extending to the single-molecule level (Rigler et al., 1993; Zander et al., 1996). This, however, requires the highest purity of solvents and solutes. Intracellular measurements based on extrinsic fluorescence probes are necessarily biased by the emission of numerous intrinsic chromophores constituting a fluorescence background (Aubin, 1979; Benson et al., 1979; Nokubo et al., 1988, 1989). In the past, fluorescence recovery after photobleaching (FRAP/FRP; Koppel et al., 1976) was the method primarily used for probing diffusion in the cytoplasm (Peters, 1983; Luby-Phelps et al., 1986; Pagliaro and Taylor, 1988), the plasma membrane (Schlessinger et al., 1977; Kusumi et al., 1993), and intracellular membranes

Received for publication 9 March 1998 and in final form 13 July 1998.

Address reprint requests to Dr. Thomas M. Jovin, Department of Molecular Biology, Max Planck Institute of Biophysical Chemistry, Am Fassberg 11, D-37077 Göttingen, Germany. Tel. +49-551-2011382; Fax: +49-551-2011467; E-mail: tjovin@mpc186.mpibpc.gwdg.de.

Mr. Hink's present address is Department of Biomolecular Sciences, Laboratory of Biochemistry, Agricultural University Wageningen, Dreyenlaan 3, 6703 HA, Wageningen, the Netherlands.

0006-3495/98/11/2547/11 $2.00

(Storrie and Kreis, 1996). The problem of ubiquitous intracellular autofluorescence was overcome by the introduction of high concentrations of exogenous fluorophores. The disadvantages of FRAP, however, include the intrinsically destructive nature of the measurement, the requirement for relatively high intracellular concentrations of fluorescent probes, and the inability to determine molecular concentrations within the observed volume element. The latter, however, is essential for understanding the thermodynamic and stochastic nature of intracellular processes. Because natural cellular chromophores are associated as cofactors with proteins as well as occurring as free low-molecular-weight compounds, their diffusion characteristics can be expected to be very similar to those of the introduced molecules.

In our measurements intracellular autofluorescence gave rise to strongly autocorrelated signals with diffusion characteristics similar to those of microinjected fluorescently labeled dextrans. The fluctuation amplitudes of these autocorrelation functions establish the lower concentration limits that can be investigated with FCM. From our studies these are on the order of a few thousand molecules per cell. Above this threshold autocorrelation functions from microinjected molecules can be detected. FCM is noninvasive and fully compatible with other forms of light microscopy, thereby allowing the delineation of the association states and interaction domains that are of central importance in intracellular signal processing and the organization of the transduction machinery.

FCS FORMALISM

Numerous publications deal with the basics of fluorescence correlation spectroscopy (e.g., Elson and Madge, 1974; Thompson, 1991). For this reason, only a short introduction will be given to the theory in general; the focus will be on the special considerations for cellular FCM.

General theory

In a system at thermodynamic equilibrium, the number of molecules of a given chemical species will fluctuate around a mean value, as represented by the normalized concentration autocorrelation function

$$G(\tau) \equiv \frac{\langle c(t)c(t+\tau)\rangle}{\langle c\rangle^2} = \frac{\langle c\rangle^2 + \langle \delta c(t)\delta c(t+\tau)\rangle}{\langle c\rangle^2} = 1 + \frac{\langle \delta c(t)\delta c(t+\tau)\rangle}{\langle c\rangle^2} \quad (1)$$

where δ denotes the deviation from the mean value $\langle c\rangle$, and τ is the temporal displacement of the signal. These number fluctuations arise by diffusion (if the observed volume is smaller than the total enclosing volume), chemical reaction, or transport processes. The relaxation of the disturbance is described by the equations defining the macroscopic process, i.e., Fick's second law for diffusion. In optical detection methods the detected signal i is not a function of the concentration fluctuation alone, but also of the optical characteristics of the instrument, and the photophysical properties of the fluorophore in situ.

FCS in multicomponent systems

In cellular FCS measurements one has to account for contributions from multiple fluorescent species representing intracellular autofluorescence (Aubin, 1979; Nuutinen, 1984; Eng et al., 1989; Schneckenburger et al., 1992), multiple labels in varying environments, and uncorrelated background fluorescence from light scatter and other sources. In contrast to conventional and confocal laser scanning fluorescence microscopy, the signal in FCS from intracellular autofluorescence and other background sources alone does not define the lower detection limit for externally introduced fluorophores (Niswender et al., 1995), but rather the number of photons per molecule. These considerations become apparent through the explicit formulation of the fluorescence intensity terms that replace the concentration terms in Eq. 1 in the case of fluorescence correlation spectroscopy. The total detected fluorescence intensity i in a system with j distinct species

$$i(t) = \sum_j i_j(t) = g \sum_j F_j \iint I(r,z)CEF(r,z)c_j \, dr \, dz \quad (2)$$

is a function of the focused illumination beam (irradiance) $I(r, z)$, the optical transfer characteristics of the detection system represented by the collection efficiency function (CEF) accounting for the fractional collection of the emitted light through the pinhole (Elson and Madge, 1974; Koppel et al., 1976; Rigler et al., 1993), an instrument factor g, and a fluorescence efficiency F_j given by the absorption and emission properties of each species:

$$F_j = \sum_k \left[n_k\sigma_k + \sum_{m\neq k} n_m\sigma_m(1 - E_{m\to k}) \right] \cdot \psi_k\gamma_k Q_k \quad (3)$$

Each species j comprises a number n_k of chromophore k with an absorption cross section σ_k (a molecular property proportional to the solution parameter ϵ, the molar extinction coefficient), a fluorescence quantum yield (in a defined reference state) Q_k, and a factor γ_k reflecting quenching by additional (to that in the reference state) processes deactivating the excited state in competition with fluorescence emission. These include self (concentration) quenching, ground-state depletion, intersystem crossing to the triplet state, resonance energy transfer, and other environment-sensitive nonradiative transitions. The factor ψ_k accounts for the wavelength dependence of the optical transmission and detector quantum efficiency in the emission band. The first term in Eq. 3 reflects direct excitation of chromophore k, and the second term (summation) indirect excitation via fluorescence resonance energy transfer (FRET; Jovin and

Arndt-Jovin, 1989; Clegg, 1995; Jares-Erijman and Jovin, 1996) from other chromophores, with transfer efficiency E. The utility of Eq. 3 derives from its unified consideration of the various fluorescence parameters accessible in the design of experimental strategies.

The global autocorrelation function $G_{tot}(\tau)$ is given as a weighted sum of a number j individual functions G_j. The analytical solution for the autocorrelation function of the detected light assumes a three-dimensional Gaussian distribution (Aragón and Pecora, 1976; Rigler et al., 1993) and can be formulated as

$$G_{tot}(\tau) = 1 + \frac{\left(1 + \frac{Te^{-\tau/\tau_T}}{1-T}\right)\left(1 - \frac{I_B}{I_{tot}}\right)^2}{N_{tot}} \cdot \sum_j \phi_j \cdot \left(\frac{1}{1+\tau/\tau_j}\right) \cdot \left(\frac{1}{1+(\omega_0^2/z_0^2)(\tau/\tau_j)}\right)^{1/2} \quad (4)$$

where the autocorrelation amplitude ($\tau = 0$) is given by

$$G_{tot}(0) = 1 + \frac{(1 + Te^{-\tau/\tau_T}/(1-T))(1 - I_B/I_{tot})^2}{N_{tot}} \cdot \sum_j \phi_j \quad (5)$$

$I_{tot} = \Sigma i_j + I_B$ is the total signal (including the uncorrelated background I_B). Uncorrelated background I_B decreases the fluctuation amplitude, i.e., it leads to a higher apparent number of molecules in the detection volume (Koppel, 1974). For each species j, F_j is the fluorescence efficiency (Eq. 3), N_j is the number of molecules in the sampled volume, and ϕ_j is the fractional weighting factor for the jth contribution to the autocorrelation function with the corresponding relative molecular fraction $Y_j = N_j/N_{tot}$.

$$\phi_j = \frac{(Y_j F_j^2)}{(\sum_j Y_j F_j)^2} \quad (6)$$

Equations 4 and 5 provide an approximate correction for the time-dependent (de)population of the triplet state, the fractional population and lifetime of which are given by T and τ_T, respectively (Widengren et al., 1995). It is a characteristic of the autocorrelation function that the relative contributions of components j in Eqs. 4 and 5 are weighted by the square of the fluorescence efficiencies. Thus a molecule with twice the fluorescence efficiency will contribute four times as much to the global autocorrelation function. The fluorescence signal per molecule (*fpm*) of species j is defined as

$$fpm_j = i_j/N_j \quad (7)$$

Intracellular FCS: approximation of local equilibria

The theory of FCS applies to systems at thermodynamic equilibrium (Elson and Madge, 1974), a condition that is not met by living cells. The concept of a local steady-state equilibrium can be applied to justify the analysis of molecular diffusibility for cells at rest or undergoing processes such as signal transduction involving changes in the association states of proteins. The use of FCS to follow nucleic acid hybridization (Oehlenschläger et al., 1996; Walter et al., 1996; Schwille et al., 1997a,b) and the binding of fluorescent ligands to receptors (Rauer et al., 1996) have demonstrated that reactions occurring in the minute range can be approximated adequately for FCS by local spatiotemporal equilibria.

FCS in small volumes: the problem of dye depletion

The measurement volume in confocal FCS is usually on the order of a femtoliter (Rigler et al., 1993). Fluctuations in the number of molecules can occur by translational diffusion only if the total volume is larger. In cuvette-type systems with microliter volumes, the dye concentration can be considered constant even if photodestruction occurs at the focus (Widengren and Rigler, 1996). This assumption has been employed in diffusion measurements by continuous microphotolysis (Peters, 1983; Kubitschek et al., 1996). The volume of a typical cell is only a few picoliters (Cassel et al., 1985; Guilak, 1994), implying that the reservoir of dye molecules is 10^{-6} that of the cuvette and that photodestruction of molecules will have an immediate impact on the signals, leading to a bias in the FCS measurement. Moreover, the average number of molecules in the observation volume no longer remains constant. Subcellular depletion of fluorescent molecules has been observed in FRAP experiments on neurons (Angelides et al., 1988). In general one seeks in FCS and FCM measurements combinations of dyes and laser irradiance that minimize photodestruction.

MATERIALS AND METHODS

Microscope

The FCM apparatus constructed in our laboratory is based on a Zeiss Axiovert 35 microscope (Carl Zeiss, Jena, Germany) with a C-Apochromat 40 × 1.2 N.A. lens to which a multichannel confocal side port with an adjustable pinhole was added (Brock et al., manuscript in preparation). The system integrates 1) positioning with resolutions and reproducibilities exceeding 1 μm along all three axes (x, y stage: Märzhäuser, Wetzlar, Germany; z-axis: Pifoc piezoelectric objective positioner, Physik Instrumente, Waldbronn, Germany); 2) high-sensitivity full-field imaging with a peltier-cooled generation-I-intensified CCD camera (HL 5; Proxitronic Funk, Bensheim, Germany); and 3) a temperature-controlled incubation chamber of local design. A 5242 Microinjector with a 5170 Micromanipulator (Eppendorf-Netheler-Hinz, Hamburg, Germany) is mounted on the microscope.

A 20-mW frequency-doubled, low-noise, single longitudinal mode, continuous-wave, Nd-YAG solid-state laser operating at 532 nm (Crysta-Laser, Reno, NV) served as the light source in all experiments. Laser power was attenuated with neutral density filters (New Focus, Santa Clara, CA) and coupled into a mono-mode fiber through a Fiber Coupler (PointSource, Winchester, England). For Cy3 excitation an XF94 DAPI-Cy3-Cy5 (Omega Optical, Brattleboro, VT) triple-path filter, in combination with a BSP560 dichroic mirror (Delta Light and Optics, Lyngby, Denmark) and

an Omega 580DF30 detection filter, was used. Fluorescence spectra were acquired with an MS125 spectrograph in an InstaSpecV detector system with a 1024 × 256 pixel CCD and a gated MCP (multichannel plate) image intensifier with three-stage peltier cooling (L.O.T. ORIEL, Darmstadt, Germany). Power densities in the focus for excitation laser light were calculated by dividing the laser power measured with a power meter (Nova Display, Ophir Optronics, Peabody, MA) by the area of the focal field, derived from the relaxation time of rhodamine 6G in PBS buffer and the reference value of the diffusion constant D (2.8×10^{-6} cm^2/s; Rigler et al., 1993).

Fluorescent probes

Amino dextrans of 10-kDa and 70-kDa molecular mass (Molecular Probes, Leiden, the Netherlands) were labeled with a 10-fold excess of the monofunctional *N*-hydroxysuccinimidyl-ester (NHS-ester) of Cy3 (Amersham Buchler, Braunschweig, Germany; Southwick et al., 1990) for 30 min at room temperature in 100 mM Na-bicine at pH 8.0. The residual reactive dye was quenched with 1 M glycine. The reacted dextran was separated from the free dye by filtration on a P2 gel filtration column (BioRad, Richmond, CA). The free dye was collected as well and used for microinjection and cuvette experiments. For mitochondrial staining, cells were incubated with 50 nM MitoTracker Green FM (Molecular Probes) in HEPES-buffered saline (HBS) (10 mM Na-HEPES, pH 7.4, 135 mM NaCl, 5 mM KCl, 1 mM $MgCl_2$, 1.8 mM $CaCl_2$, 1% glucose, and 0.1% BSA) for 30 min.

Cells

A431 human epidermoid carcinoma cells (Fabricant et al., 1977) and the human epidermal growth factor receptor (EGFR)-expressing, National Institutes of Health-3T3 fibroblast-derived murine cell line Her14 (Honegger et al., 1988) were grown in a 5% CO_2 humidified atmosphere at 37°C in Dulbecco's modified Eagle medium (DMEM) supplemented with 10% FCS, 10^4 units/liter penicillin G, and 100 mg/liter streptomycin sulfate. For FCM experiments, cells were grown to subconfluency on 12-mm glass coverslips and mounted in the incubation chamber on the microscope stage in HBS. The temperature in the chamber was kept at 37°C by perfusion through an outer heating ring.

Intracellular FCM of microinjected molecules

Before microinjection, samples were centrifuged for 10 min at 90,000 × g in an Airfuge ultracentrifuge (Beckman Instruments, Palo Alto, CA). Cells were microinjected on the FCM with Eppendorf Femtotips. Individual cells were selected in the transmission image. To localize the cell along the optical axis, the laser focus was scanned through the cell. Reference autocorrelation functions of the intracellular autofluorescence were recorded before microinjection. In addition, autocorrelation functions were recorded 50 μm above the cell in the incubation buffer before and after microinjections. These functions were not affected by the microinjection and were used to verify the stability of the system during the measurements. After microinjection another z-profile was recorded to confirm that the cell was microinjected. Two additional z-profiles at 3 and 6 min after microinjection were acquired to check for leakage of the dye out of the cell. If the signal was stable, intracellular autocorrelation measurements were carried out. The measurement time was 30 s in each case.

Data analysis

Autocorrelation functions were acquired on-line with the ALV 5000 dual-channel correlator board (ALV, Langen, Germany) and saved as ASCII files. The correlation curves were analyzed with macros using the Marquardt-Levenberg algorithm (Marquardt, 1963) and implemented in Igor Pro (WaveMetrics, Lake Oswego, OR) on an Apple Power Macintosh computer. The triplet state lifetime τ_T, triplet fraction T, the fractions ϕ_j, and the characteristic diffusion times τ_j of components j where allowed to vary for the fitting. The structure factor (ω_0/z_0) was 1/4, where ω_0 is the radius of the detection volume in the focal plane and z_0 is the extension along the optical axis. Diffusion constants D were calculated from autocorrelation times according to $\tau = \omega_0^2/4D$.

RESULTS

Autocorrelations were observed in cellular measurements using 532-nm laser excitation in the absence of any extrinsic label. To define the conditions for intracellular FCM in the presence of such intrinsic autocorrelations, we directed our studies toward a characterization of intracellular autofluorescence according to Eq. 3, and then to the determination of the sensitivity limits for the detection of an extrinsic fluorescently labeled model compound. A new method was devised to analyze molecular association based on the combination of molecule numbers derived from the fluorescence signal per molecule (*fpm*) and the autocorrelation amplitude.

Characterization of intracellular autofluorescence autocorrelations

Autocorrelation functions

Her14 is a mouse National Institutes of Health-3T3 fibroblast-derived cell line, and A431 is a human epidermoid carcinoma cell line. Both cell lines exhibited intracellular autofluorescence upon excitation at 532 nm, leading to a well-defined autocorrelation function. To ensure that these autocorrelations did not arise from vibrations of the on-stage perfusion system or other elements of the microscope, a coverslip coated with a thin fluorescent film (kindly provided by Stephan Hell) was measured, showing no autocorrelations (data not included). The detection window was selected for Cy3 fluorescence. Three component fits were sufficient to describe the data (Fig. 1). No triplet component was apparent in measurements of intracellular autofluorescence at low laser intensities around 5 kW/cm. At higher laser powers the inclusion of a triplet term clearly improved the quality of the fits.

Origin of autofluorescence and spectral characterization

Imaging with the digital camera was carried out with excitation at 546 nm and detection of the fluorescence through the same emission filters used with laser illumination. The autofluorescence colocalized strongly within mitochondria, identified by their characteristic morphology and the MitoTracker Green fluorescent dye (Fig. 2, *A–C*). The fluorescence emission spectrum of Cy3 was nearly identical to the autofluorescence in the window of the emission filter (Fig. 2 *D*).

Change of intracellular autofluorescence with time

Time-lapse video microscopy of cells incubated at 37°C in HBS supplemented with 0.1% BSA and 1% glucose dem-

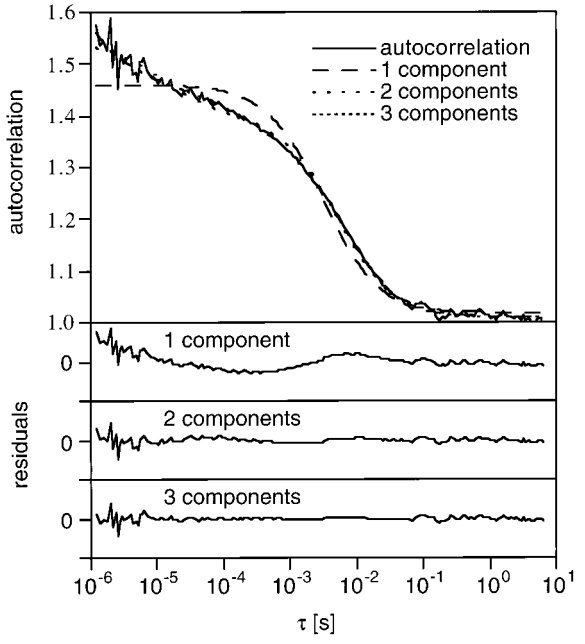

FIGURE 1 Fits with one, two, or three diffusing components to an intracellular autofluorescence autocorrelation function, and corresponding residuals. The one-component fit reproduced the major contribution at long relaxation times. The three-component fit yielded satisfactory results over the whole autocorrelation function. In each case the range of the residuals is ±0.15.

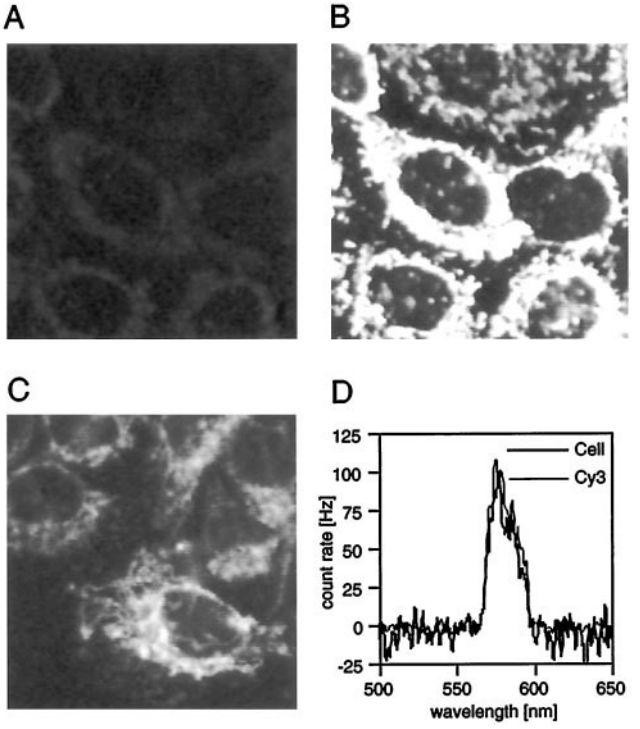

FIGURE 2 Intracellular distribution of autofluorescence in A431 cells. (*A*) At the beginning of the experiment little autofluorescence was detected. (*B*) Intracellular autofluorescence after incubation for 90 min on the microscope stage at 37°C. The autofluorescence strongly localized to mitochondrial structures. (*C*) A431 cells stained with the mitochondrial dye MitoTracker Green FM. (*D*) Comparison of the fluorescence emission spectra of the indocyanine dye Cy3 and intracellular autofluorescence detected through a 580DF30 bandpass filter. Cy3 differed from the intracellular autofluorescence by a slightly greater fluorescence emission at shorter wavelengths. The concentration of Cy3 was 10 nM, and the laser power was 7 kW/cm at a pinhole size of 100 μm, with 3-s integration and averaging over two measurements. The Cy3 spectra was scaled to fit the autofluorescence intensity, and both spectra were smoothed with a low-pass filter. The spectra were not corrected for the transmission characteristics of the optical system.

onstrated a strong increase in mitochondrial autofluorescence (Fig. 2, *A–C*). The dependence of intracellular autocorrelation functions on the time of incubation on the microscope stage was investigated for two A431 and two HER14 cells under the same conditions. Every 5 min over an 80-min period, an autocorrelation function was measured at the same subcellular location for 60 s with a laser power of 7 kW/cm. The cells were exposed to the laser light only during the measurements. In all cases an increase in the intracellular autofluorescence by a factor of 4–8 was observed (Fig. 3). This effect was even more pronounced when the cells were incubated at room temperature (data not shown). The A431 and Her14 cells were indistinguishable. To evaluate whether the evolution of the signal resulted from an increase in the number of fluorescent particles or from an increase in the fluorescence signal per molecule (*fpm*), the fluorescence count rates were divided by the number of molecules obtained from the autocorrelation amplitudes for each time point (Fig. 3 *B*); *fpm* but not *N* increased in all cases. After the addition of 20 mM sodium sulfite (pH 7.4), used as a reducing agent for intracellular autofluorescence (Nokubo et al., 1988), the fluorescence returned to its starting values within a few minutes (data not shown).

Dependence of intracellular autofluorescence autocorrelations on excitation laser power

The dependence of the intracellular autofluorescence on excitation laser power was studied in the nucleus and in the cytoplasm of Her14 cells. Because the nucleus differs profoundly in chemical and structural terms from the cytoplasm and its components, the sensitivity of FCS in measuring autocorrelations for microinjected molecules might differ in these subcellular locations. The intranuclear autofluorescence increased more strongly with laser power than the cytoplasmic autofluorescence, reaching a plateau at 5 kW/cm (Fig. 4 *A*). The autocorrelation functions were fitted with three components, including a triplet term for all but the lowest laser power. Except for one cell, the number of molecules decreased as the laser power was increased from 2–7 kW/cm and remained constant at higher power densities (Fig. 4 *B*).

In multicomponent systems consisting of molecules with different diffusion constants but carrying the same fluorophore, the slowest have the highest likelihood of bleaching, because they reside the longest in the illuminated volume. As a consequence, the apparent composition of the ensemble will change with increasing laser power. To investigate

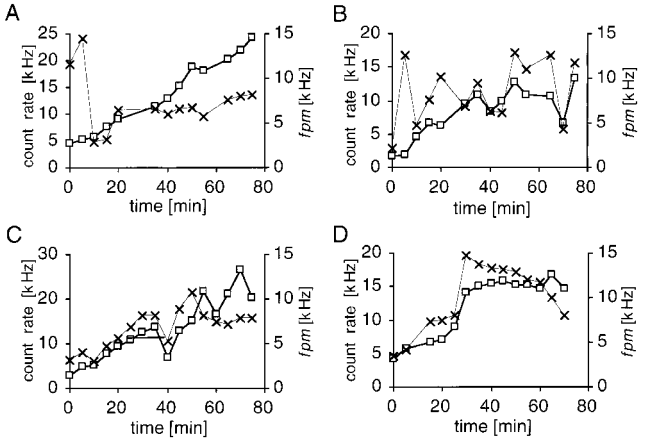

FIGURE 3 Time dependence of intracellular autofluorescence levels for two HER14 cells (*A* and *B*) and two A431 cells (*C* and *D*). The total autofluorescence count rate is given on the primary axis (□), the fluorescence signal per molecule (*fpm*) on the secondary axis (×). In all cases an increase in the count rate was observed, which in *C* and *D* strongly correlated with an increase in *fpm*, indicating that a conversion from molecular species with low fluorescence efficiency to another species with higher efficiency had occurred. It cannot be excluded that sudden variations (*A* and *B*) were partially due to intracellular motions during incubations so that autofluorescence from other compartments was detected. The excitation wavelength was 532 nm, and fluorescence was detected over 565–595 nm. In all cases the fluorescence increased with time.

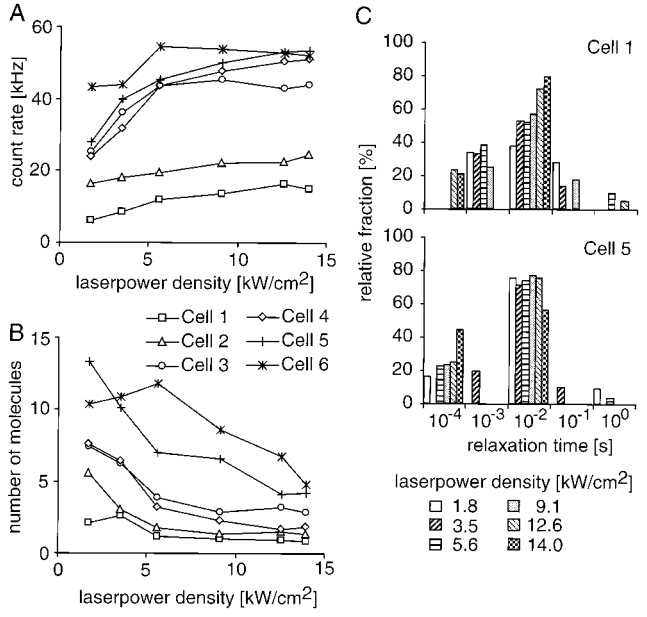

FIGURE 4 Dependence of intracellular autofluorescence and autocorrelations on excitation laser power and subcellular location in Her14 cells. (*A*) Photodetector count rates at increasing excitation laser power density for cytoplasmic (*Cells 1–3*) and nuclear (*Cells 4–6*) autofluorescence. Except for one case of cytoplasmic autofluorescence (*Cell 3*), the nuclear autofluorescence increased more strongly and reached a plateau at 5–10 kW/cm. (*B*) The dependence of the number of molecules on the excitation power calculated from the autocorrelation functions. A significant decrease in the number of molecules was observed in all but one case (*Cell 1*). For the intranuclear measurements of Cells 5 and 6, two to three times as many molecules were present as for the cytoplasmic compartments. Measurements for microinjected materials were carried out at a laser power density of 7 kW/cm. (*C*) Dependence of the contributions of fast and slow relaxation times to the autocorrelation functions on laser power. Shown here are two examples out of a total of six. The autocorrelation functions were fitted with three-component models that included a triplet term. In some cases, two of the components had nearly identical relaxation times or were both within the interval of one decadic bin. The percentage contribution of each component to the autocorrelation function is plotted versus the relaxation time. The labels correspond to the lower limits of the decadic intervals.

if such an effect applied to the intracellular autofluorescence, the relative fraction of each component was plotted versus the autocorrelation time (Fig. 4 *C*). As expected, the fraction of the slowly diffusing component decreased in most cases, and that of the fast diffusing component increased. In many cases, these characteristic diffusion times were faster than expected for a low-molecular-weight compound in our FCM. Apparently, despite the inclusion of a triplet term (not shown in the graphs), the fits did not separate the triplet relaxation times fully from diffusion processes. Systematic differences were not found upon comparing the cytoplasmatic and nuclear autocorrelation functions. For both locations, some of the measurements showed very slow contributions in the lower second range, and in others autocorrelation times in the upper millisecond range were lacking. The most prominent autocorrelation time was 5–10 ms.

Intracellular measurements with microinjected Cy3 dextran

In a multicomponent system consisting of intracellular autofluorescence and injected fluorescently labeled compounds, the fluorescence signal per molecule fpm_j (Eq. 3) determines the contribution of the molecule to the total autocorrelation function (Eqs. 4–6). For a dilution series of free Cy3, Cy3-labeled 10 kDa dextran and 70 kDa dextran, and for intracellular autofluorescence the photodetector count rate was plotted versus the number of molecules obtained from the autocorrelation functions (Fig. 5). The relative *fpm*, normalized to the value of the free dye, were calculated from the ratios of the slopes (Table 1). The value for the 10-kDa Cy3 dextran was twice, and the 70 kDa dextran and the intracellular autofluorescence five times that of the free dye.

For intracellular FCM measurements the 10-kDa Cy3-labeled dextran was chosen for two reasons. First, according to data derived from FRAP measurements (Peters, 1984), this molecule was expected to have a relaxation time shorter than the 5–10 ms of the major component of the intracellular autofluorescence. Second, the dextran carried, on average, two dyes per molecule, as determined from the relative fluorescence efficiencies. For proteins, low labeling ratios are preferred to preserve function. Intracellular measurements were performed at power densities of 7 kW/cm, because for this value the contribution of the intracellular autofluorescence to the autocorrelation was reduced (Fig. 4 *B*), but bleaching was still minimal. The autocorrelation

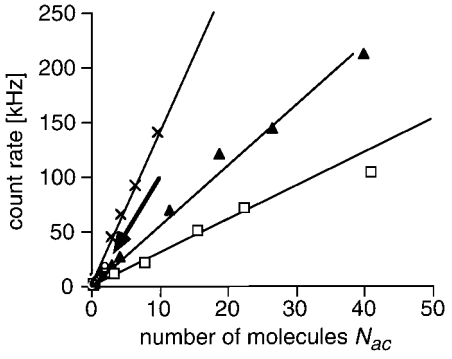

FIGURE 5 Fluorescence signals for Cy3, Cy3-labeled 10 kDa and 70 kDa dextrans and intracellular autofluorescence. □, Free Cy3; ▲, 10 kDa Cy3 dextran; ×, 70 kDa Cy3 dextran; ○, autofluorescence. The number of molecules N_{ac} obtained through fits of the autocorrelation functions correlated linearly with the count rate. The free Cy3 dye had the smallest slope. The values for the autofluorescence were from a time series of a Her14 cell (*arrow*). The slope was comparable to the 70-kDa dextran (Table 1).

functions before and after microinjection were analyzed with a three-component algorithm containing a triplet term where necessary (Eq. 4 and Fig. 6). For data analysis, the weighting factors ϕ_j (Eq. 6) were not decomposed into their components, because the time and position dependence of the autofluorescence prohibited the assignment of a relative fluorescence efficiency with high precision. In addition, the signal of the microinjected molecules was expected to dominate the autocorrelation function because of the low number of intracellular autofluorescent molecules.

For many microinjected cells, the changes in the number of molecules ΔN_{ac} for each microinjection obtained from the autocorrelation amplitudes before and after microinjection were plotted against the number of molecules obtained from the increase in the fluorescence count rates, ΔN_c (Fig. 7 *A*). The latter quantity was obtained by dividing the total increase in count rate by the fluorescence signal per molecule (*fpm*) derived from cuvette measurements of the dextran. For a total of 35 microinjected cells, the average number of molecules before microinjection was 1.2 ± 1.6, with a minimum of 0.2 and a maximum of 9.4. The greatest increase in the number of molecules within the observation volume was 330. In a few cases, decreases in the number of molecules were observed, possibly due to dilution effects or distortions of the subcellular structure (data not shown). At lower levels of microinjected molecules, only increases in the fluorescence count rate were observed. When more molecules were microinjected, ΔN_{ac} correlated positively with ΔN_c. A linear regression applied to all data points resulted in a slope of 0.99 (R^2 0.96). The autocorrelation times after microinjection were plotted against $\Delta N_{ac}/\Delta N_c$ (Fig. 7 *B*). A ratio close to unity signifies that the microinjected molecules were freely diffusible, whereas a ratio less than 1 indicates that the molecules were either bound to intracellular structures or confined in their movement within the detection volume. As can be seen, for ratios of ~1 the autocorrelation time was ~3 ms. For smaller ratios, the autocorrelation times were more scattered and were as high as 13 ms.

The sensitivity of intracellular measurements is defined by the minimum number of molecules that have to be introduced into the cells to detect freely diffusible molecules. To address this question, the autocorrelation times after microinjection were plotted versus ΔN_c and ΔN_{ac}, respectively (Fig. 7, *C* and *D*). ΔN_c represents an absolute measure of the number of molecules, whereas ΔN_{ac} identifies freely diffusible molecules. In the two cases where more than 250 dextran molecules were present in the detection volume, autocorrelation times of less than 3 ms were found. The autocorrelation analysis demonstrated that as soon as more than 25 molecules were detected, the derived diffusion constants were appropriate for freely diffusible molecules.

TABLE 1 Relative fluorescence signals per molecule (*rfpm*) for Cy3-labeled molecules and intracellular autofluorescence

Fluorophore	*rfpm*	Diffusion constant D (cm^2/s)
Free Cy3	1.0 ± 0.1	2.8×10^{-6}
10-kDa Cy3 dextran	2.1 ± 0.2	7.0×10^{-7}
70-kDa Cy3 dextran	5.0 ± 0.5	3.0×10^{-7}
Her14 autofluorescence	5.3 ± 3.2	—

Relative fluorescence signals per molecule *rfpm* for Cy3-labeled molecules and intracellular autofluorescence. Given are the averages for the relative slopes from two independent experiments (Fig. 5). The diffusion constants were derived from the autocorrelation times as described in Materials and Methods.

DISCUSSION

We have implemented fluorescence correlation microscopy (FCM) and characterized its performance by the measurement of intracellular diffusion of a microinjected fluorescent dextran in the presence of high-autofluorescence backgrounds. In contrast to established techniques like FRAP, FCM requires that low numbers of molecules can be specifically detected. The first part of our analysis, therefore, has served to define the "boundary conditions" imposed by the autofluorescence background on intracellular FCM.

Characterization of intracellular autofluorescence

In all of our measurements strong autocorrelations arising from intracellular autofluorescence were observed. This finding is in contrast to experiments reported by Berland et al. (1995) with 7-nm fluorescent latex microspheres and two-photon excitation (Denk et al., 1990), in which intracellular autocorrelations were absent. Diffusion of microspheres into and out of the sample volume results in much larger fluctuation amplitudes. For this reason it is very possible that autocorrelations could not be detected in two-photon excitation for the intracellular autofluorescence. Using thin fluorescent films with immobilized fluorophores,

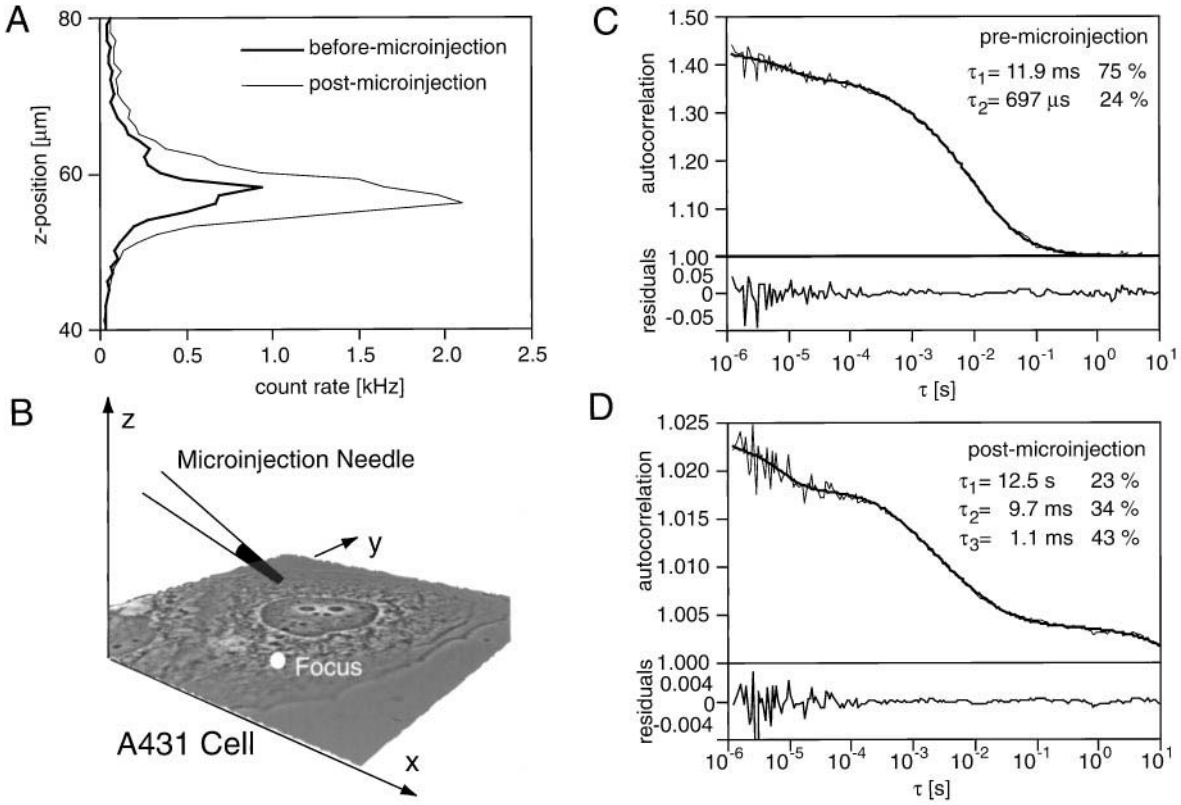

FIGURE 6 Intracellular FCS of Cy3-labeled 10-kDa dextran for a representative case. (*A*) Profiles of the count rate along the optical axis before and after microinjection recorded at low laser power (4 kW/cm^2) by automatically focusing through the cell. In this way, the focus was localized precisely and the integrity of the cell was assessed. (*B*) Three-dimensional representation of the experimental setup. (*C*, *D*) Autocorrelation functions and their analyses before and after microinjection.

we confirmed that the fluctuations were not introduced by our instrument. Digital imaging microscopy detected a large temporal increase in the mitochondrial autofluorescence that correlated with an increase in the fluorescent count rate in the autocorrelation measurements. The further characterization of the intracellular autofluorescence demonstrated the presence of multiple components. The autocorrelation amplitude corresponded to only 0.2–10 molecules in a detection volume of ~1 fl, corresponding to 0.3–15 nM or 800–40,000 molecules in a cell with a total volume of 4 pl. The relative fluorescence signal, however, was surprisingly high, considering that neither NAD nor FAD absorbs strongly at the excitation wavelength of 532 nm. However, the emission spectrum of the intracellular autofluorescence matched the spectra reported for intracellular flavins and flavoproteins (Aubin, 1979; Benson et al., 1979; Nokubo et al., 1988, 1989). Porphyrins can be excluded as an alternative source of autofluorescence, because their emission is present only after incubation with the precursor δ-aminolevulinic acid in A431 cells (He et al., 1993), and in addition differs from the recorded spectra. The fact that the autofluorescence was decreased by reducing agents added further evidence for the existence of flavins (Nokubo et al., 1988). The increase in autofluorescence was partially due to an increase in the fluorescence signal per molecule (*fpm*). In addition, an increase in the number of molecules was observed in most cases. This effect could have reflected either subcellular motions or an increase in the fluorescence signals of certain molecules above the detection threshold because of metabolism-dependent changes in their quantum yields.

The high fluctuation amplitude (i.e. low number of molecules), the high relative fluorescence signal per molecule, and the colocalization of the autofluorescence with the mitochondria point to molecular aggregates or subcellular structures as the source of autofluorescence autocorrelations. The autocorrelations would then arise from concerted motions of large numbers of fluorophores. Diffusion constants of 1×10^{-7} cm^2/s to 5×10^{-8} cm^2/s were found for the 160-kDa protein aldolase in different subcellular locations (Pagliaro and Taylor, 1988). In our FCM this value corresponded to relaxation times of 5–10 ms. It is important to note that no simple inverse relationship exists between the hydrodynamic radius of a protein and its diffusion rate in the cytoplasm, because translational motion is hindered by the meshwork of the cytoskeleton (Luby-Phelps et al., 1986, 1987). Because it was impossible to assign the autofluorescence to a distinct molecular species and in light of the evidence for a mitochondrial origin, it seems more appropriate to talk of fluorescent entities rather than molecules.

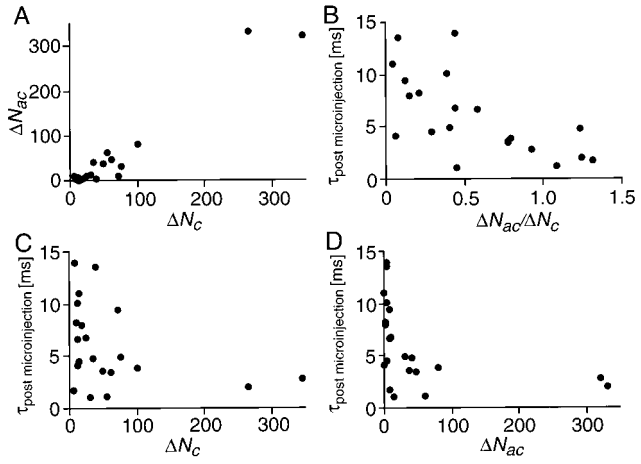

FIGURE 7 Analysis of the diffusibility of microinjected 10-kDa Cy3 dextran with FCS. (*A*) Plot of the number of microinjected molecules obtained from the change in the autocorrelation amplitude ΔN_{ac} versus the number of molecules calculated from the increase in photodetector count rate ΔN_c. Each data point represents one intracellular measurement. Values on a line with unit slope would indicate free diffusibility of the injected molecules. (*B*) Secondary plot of the relaxation time of the major component in the autocorrelation functions versus the ratio of the number of molecules from both calculations. For ratios of ~1, the relaxation time approached values consistent with data from other techniques. (*C* and *D*) Plots of the number of molecules from both determinations versus relaxation time. Only if the number of injected molecules derived from the change in the autocorrelation amplitude exceeded 25 did the relaxation times approach the value corresponding to freely diffusible molecules. The data for microinjected Her14 cells were indistinguishable from those for A431 cells.

FCS offers new insight into the metabolic phenomena that underlie autofluorescence (Schneckenburger et al., 1992; Leyssens et al., 1996). It can distinguish between spectral changes of existing fluorophores and the generation of new fluorophores. From the autocorrelation functions one can infer whether the fluorophores are present as high- or low-molecular-weight species. Simultaneous measurements of fluorescence spectra, as have been carried out with our instrument, further define the nature of the molecules in question. The photophysical properties of the autofluorescence of mammalian cells depended on the subcellular location. The number and diffusion times of the entities clustered around certain values but were still too heterogeneous to derive common parameters that could serve as references for intracellular measurements in general. However, we have shown that the autofluorescence background can be tuned by the selection of spectral ranges, excitation powers, and incubation conditions to optimize the sensitivity for the extrinsic fluorophore.

Measurement of microinjected Cy3 dextran

Autocorrelation functions were measured before and after microinjection of a Cy3-labeled dextran into A431 and HER14 cells. Photobleaching was not a problem in our intracellular measurements. For FCS in cuvettes, the molecules within the observation focus are recruited from a virtually unbounded reservoir. Under these circumstances it has been possible to study the effects of photodestruction on the correlation times (Widengren and Rigler, 1996). In these cases, however, only 10^{-6} of the total number of molecules were in the focus of the laser beam at the same time. In contrast, intracellular FCM faces the problem of dye depletion due to the small total volume in which the measurement takes place. The probability of photodestruction will increase as the diffusion constant decreases. However, for the observation of processes with slower relaxation times, the laser power can be lowered because the signal-to-noise ratio in FCS is determined by the number of photons per molecule per residence time (Qian, 1990). In this way, a separation of the dye depletion time constants from the relaxation time constants can be maintained to the limit defined by the dark count rate of the photodetector.

The number of Cy3-labeled dextran molecules that were microinjected into a cell were independently determined in two ways. The first calculation was based on the increase in the photodetector count rate. For this determination the count rate per molecule in solution at a given excitation laser power was measured with FCS. Second, the number was obtained from the intracellular autocorrelation amplitudes before and after microinjection. When low numbers of molecules (<25 in the detection volume) where injected, there was a discrepancy between the two numbers. Only with more than 25 injected molecules in the detection volume was the plot of ΔN_c and ΔN_{ac} linear. A fit according to Eq. 5 was unable to describe the data. Because the intracellular autofluorescence corresponded to low numbers of fluorescent entities, a much higher relative fluorescence efficiency than experimentally determined had to be assumed. In view of the high autocorrelation amplitude, an uncorrelated fluorescence background as a source of this behavior was unlikely. We conclude that the observation was probably due to a local confinement or interaction of the dextran with intracellular structures. Because FCM operates at lower molecule concentrations than FRAP, no direct comparison of our observations with other reported data is possible at this time.

Consistent with the interpretation that the molecules were freely diffusible if $\Delta N_{ac}/\Delta N_c \approx 1$, the diffusion constants agreed well with those reported earlier from intracellular FRAP measurements. The diffusion constant of rhodamine 6G in water measured with FCS is 2.8×10^{-6} cm^2/s. In our instrument, we determined an autocorrelation time of 180 μs. An autocorrelation time of 2.9 $\pm$ 1.2 ms for the 10-kDa dextran (average of values with $\Delta N_{ac}/\Delta N_c > 0.7$; Fig. 7 *B*) corresponds to a diffusion constant of 1.7×10^{-7} cm^2/s. Peters determined the diffusion constant for a 10-kDa dextran in solution as 7.6×10^{-7} cm^2/s (Peters, 1984). For a Ficoll fraction with a radius of 32 Å, which is comparable to the 10-kDa dextran (Peters, 1984), a relative diffusion constant (cytoplasm to free solution) of 0.277 has been reported (Luby-Phelps et al., 1987). Taken together, the expected value for the diffusion constant of a 10-kDa dex-

TABLE 2 Comparison of intracellular diffusion constants for 10-kDa dextrans measured with FRAP and FCM

Method	Diffusion constant D (cm^2/s)
FRAP I*	2.1×10^{-7}
FRAP II#	1.9×10^{-7}
FCM	1.7×10^{-7}

*Combined data from Peters (1984) (diffusion constant of a 10-kDa dextran in solution) and Luby-Phelps et al. (1987) (relative diffusibility of a similar solute in the cytoplasm).
#Luby-Phelps et al. (1986).

tran from FRAP in the cytoplasm is 2.1×10^{-7} cm^2/s. In an earlier paper Luby-Phelps et al. (1986) gave the diffusion constant for a 10-kDa dextran in the cytoplasm as 1.9×10^{-7} cm^2/s (Luby-Phelps et al., 1986; Table 2). These values agree very well with the diffusion constant that we measured by FCM. However, it is important to note that the analysis of association states with FCM does not necessarily depend on diffusion rate constants. It is possible to determine the association from the slope of the $\Delta N_{ac}/\Delta N_c$ plot (Fig. 7 *A*), thereby exploiting the unique capability of FCM for measuring absolute molecule numbers.

FCS traditionally has been a technique for the measurement of diffusibility and photophysical properties of low numbers of molecules in very well-defined systems in solution. For measurements with microinjected molecules, fluorophores can be chosen that emit in the near infrared (Southwick et al., 1990) and thus avoid background contributions in cell biological applications. Initial experiments with our instrument have indicated that no intracellular autocorrelations were present in our cell lines at excitation at 633 nm. However, increasing attention has been focused in the past few years on the use of GFP fusion proteins (Prasher et al., 1992; Chalfie et al., 1994; Niswender et al., 1995) as fluorescent probes for intracellular localization, trafficking (Kaether and Gerdes, 1995; Presley et al., 1997), and protein mobility (Westphal et al., 1997). That GFP can serve as a probe for FCS has already been demonstrated in solution (Terry et al., 1995; Brock et al., manuscript in preparation). For GFP and its mutants, however, the longest excitation wavelengths are still very close to 500 nm (Heim and Tsien, 1996; Miyawaki et al., 1997), a range where autofluorescence cannot be avoided. The protocols that we developed here establish the feasibility of intracellular FCM in the presence of autofluorescence autocorrelations. With this foundation, FCM also benefits from the versatility of this fluorophore (Brock and Jovin, submitted manuscript). For GFP as well, reference measurements with free GFP in solution provide reliable data on the absolute numbers of molecules.

Roland Brock is the recipient of a fellowship from the Studienstiftung des deutschen Volkes.

We thank Christian Eggeling, Claus Seidel, and Petra Schwille for helpful discussions.

REFERENCES

Angelides, K. J., L. W. Elmer, D. Loftus, and E. Elson. 1988. Distribution and lateral mobility of voltage-dependent sodium channels in neurons. *J. Cell Biol.* 106:1911–1925.

Aragón, S. R., and R. Pecora. 1976. Fluorescence correlation spectroscopy as a probe of molecular dynamics. *J. Chem. Phys.* 64:1791–1803.

Aubin, J. E. 1979. Autofluorescence of viable cultured mammalian cells. *J. Histochem. Cytochem.* 27:36–43.

Benson, R. C., R. A. Meyer, M. E. Zaruba, and G. M. McKhann. 1979. Cellular autofluorescence—is it due to flavins? *J. Histochem. Cytochem.* 27:44–48.

Berland, K. M., P. T. C. So, and E. Gratton. 1995. Two-photon fluorescence correlation spectroscopy: method and application to the intracellular environment. *Biophys. J.* 68:694–701.

Berland, K. M., P. T. C. So, Y. Sen, W. W. Mantulin, and E. Gratton. 1996. Scanning two-photon fluctuation correlation spectroscopy: particle counting measurements for detection of molecular aggregation. *Biophys. J.* 71:410–420.

Brock, R., and T. M. Jovin. 1998. Fluorescence correlation microscopy (FCM)—FCS taken into the cell. *Cell. Mol. Biol.* 44:847–856.

Cassel, D., B. Whiteley, Y. X. Zhuang, and L. Glaser. 1985. Mitogen-independent activation of Na^+/H^+ exchange in human epidermoid carcinoma A431 cells: regulation by medium osmolarity. *J. Cell. Phys.* 122:178–186.

Chalfie, M., Y. Tu, G. Euskirchen, W. W. Ward, and D. C. Prasher. 1994. Green fluorescent protein as a marker for gene expression. *Science.* 263:802–805.

Clegg, R. M. 1995. Fluorescence resonance energy transfer. *Curr. Opin. Biotechnol.* 6:103–110.

Denk, W., J. H. Strickler, and W. W. Webb. 1990. Two-photon laser scanning fluorescence microscopy. *Science.* 248:73–76.

Elson, E. L., and D. Madge. 1974. Fluorescence correlation spectroscopy. I. Conceptual basis and theory. *Biopolymers.* 13:1–27.

Eng, J., R. M. Lynch, and R. S. Balaban. 1989. Nicotinamide adenine dinucleotide fluorescence spectroscopy and imaging of isolated cardiac myocytes. *Biophys. J.* 55:621–630.

Fabricant, R. N., J. E. D. Larco, and G. J. Todaro. 1977. Nerve growth factor receptors on human melanoma cells in culture. *Proc. Natl. Acad. Sci. USA.* 74:565–569.

Fahey, P. F., D. E. Koppel, L. S. Barak, D. E. Wolf, E. L. Elson, and W. W. Webb. 1977. Lateral diffusion in planar lipid bilayers. *Science.* 195: 305–306.

Guilak, F. 1994. Volume and surface area measurement of viable chondrocytes in situ using geometric modelling of serial confocal sections. *J. Microsc.* 173:245–256.

He, D., S. Sassa, and H. W. Lim. 1993. Effect of UVA and blue light on porphyrin biosynthesis in epidermal cells. *Photochem. Photobiol.* 57: 825–829.

Heim, R., and R. Y. Tsien. 1996. Engineering green fluorescent protein for improved brightness, longer wavelengths and fluorescence resonance energy transfer. *Curr. Biol.* 6:178–182.

Honegger, A., T. J. Dull, F. Bellot, E. V. Obberghen, D. Szapary, A. Schmidt, A. Ullrich, and J. Schlessinger. 1988. Biological activities of EGF-receptor mutants with individually altered autophosphorylation sites. *EMBO J.* 7:3045–3052.

Jares-Erijman, E., and T. M. Jovin. 1996. Determination of DNA helical handedness by fluorescence resonance energy transfer. *J. Mol. Biol.* 257:596–617.

Jovin, T. M., and D. J. Arndt-Jovin. 1989. FRET microscopy: digital imaging of fluorescence resonance energy transfer. Application in cell biology. *In* Cell Structure and Function by Microspectrofluorometry. Academic Press, London. 99–117.

Kaether, C., and H.-H. Gerdes. 1995. Visualization of protein transport along the secretory pathway using green fluorescent protein. *FEBS Lett.* 369:267–271.

Koppel, D. E. 1974. Statistical accuracy in fluorescence correlation spectroscopy. *Phys. Rev. A.* 10:1938–1945.

Koppel, D. E., D. Axelrod, J. Schlessinger, E. L. Elson, and W. W. Webb. 1976. Dynamics of fluorescence marker concentrations as a probe of mobility. *Biophys. J.* 16:1315–1329.

Kubitschek, U., O. Heinrich, and R. Peters. 1996. Continuous scanning microphotolysis: a simple laser scanning microscopic method for lateral transport measurements employing single- or two-photon excitation. *Bioimaging.* 4:158–167.

Kusumi, A., Y. Sako, and M. Yamamoto. 1993. Confined lateral diffusion of membrane receptors as studied by single particle tracking (nanovid microscopy). Effects of calcium-induced differentiation in cultured epithelial cells. *Biophys. J.* 65:2021–2040.

Leyssens, A., A. V. Nowicky, L. Patterson, M. Crompton, and M. R. Duchen. 1996. The relationship between mitochondrial state, ATP hydrolysis, $[Mg^{2+}]_i$ and $[Ca^{2+}]_i$ studied in isolated rat cardiomyocytes. *J. Physiol. (Lond.).* 496.1:111–128.

Luby-Phelps, K., P. E. Castle, L. Taylor, and F. Lanni. 1987. Hindered diffusion of inert tracer particles in the cytoplasm of mouse 3T3 cells. *Proc. Natl. Acad. Sci. USA.* 84:4910–4913.

Luby-Phelps, K., D. L. Taylor, and F. Lanni. 1986. Probing the structure of cytoplasm. *J. Cell Biol.* 102:2015–2022.

Madge, D., E. Elson, and W. W. Webb. 1972. Thermodynamic fluctuations in a reacting system-measurement by fluorescence correlation spectroscopy. *Phys. Rev. Lett.* 29:705–708.

Madge, D., E. L. Elson, and W. W. Webb. 1974. Fluorescence correlation spectroscopy. II. An experimental realization. *Biopolymers.* 13:29–61.

Maiti, S., U. Haupts, and W. W. Webb. 1997. Fluorescence correlation spectroscopy: diagnostics for sparse molecules. *Proc. Natl. Acad. Sci. USA.* 94:11753–11757.

Marquardt, D. W. 1963. An algorithm for least-squares estimation of nonlinear parameters. *J. Soc. Indust. Appl. Math.* 11:431–441.

Miyawaki, A., J. Llopis, R. Heim, J. M. McCafferty, J. A. Adams, M. Ikura, and R. Y. Tsien. 1997. Fluorescent indicators for Ca^{2+} based on green fluorescent proteins and calmodulin. *Nature.* 388:882–887.

Niswender, K. D., S. M. Blackman, L. Rohde, M. A. Magnuson, and D. W. Piston. 1995. Quantitative imaging of green fluorescent protein in cultured cells: comparison of microscopic techniques, use in fusion proteins and detection limits. *J. Microsc.* 180:109–116.

Nokubo, M., M. Ohta, K. Kitani, and I. Zs.-Nagy. 1989. Identification of protein-bound riboflavin in rat hepatocyte plasma membrane as a source of autofluorescence. *Biochim. Biophys. Acta.* 981:303–308.

Nokubo, M., I. Zs.-Nagy, K. Kitani, and M. Ohta. 1988. Characterization of the autofluorescence of rat liver plasma membranes. *Biochim. Biophys. Acta.* 939:441–448.

Nuutinen, E. M. 1984. Subcellular origin of the surface fluorescence of reduced nicotinamides in the isolated perfused rat heart. *Basic Res. Cardiol.* 79:49–58.

Oehlenschläger, F., P. Schwille, and M. Eigen. 1996. Detection of HIV-1 RNA by nucleic acid sequence-based amplification combined with fluorescence correlation spectroscopy. *Proc. Natl. Acad. Sci. USA.* 93: 12811–12816.

Pagliaro, L., and D. L. Taylor. 1988. Aldolase exists in both the fluid and solid phases of cytoplasm. *J. Cell Biol.* 107:981–991.

Palmer, A. G. I., and N. L. Thompson. 1987. Molecular aggregation characterized by high order autocorrelation in fluorescence correlation spectroscopy. *Biophys. J.* 52:257–270.

Peters, R. 1983. Fluorescence microphotolysis. Diffusion measurements in single cells. *Nature.* 70:294–302.

Peters, R. 1984. Nucleo-cytoplasmic flux and intracellular mobility in single hepatocytes measured by fluorescence microphotolysis. *EMBO J.* 3:1831–1836.

Prasher, D. C., V. K. Eckenrode, W. W. Ward, F. G. Prendergast, and M. J. Cormier. 1992. Primary structure of the *Aequorea victoria* green-fluorescent protein. *Gene.* 111:229–233.

Presley, J. F., N. B. Cole, T. A. Schroer, K. Hirschberg, K. J. M. Zaal, and J. Lippincott-Schwartz. 1997. ER-to-Golgi transport visualized in living cells. *Nature.* 389:81–85.

Qian, H. 1990. On the statistics of fluorescence correlation spectroscopy. *Biophys. Chem.* 38:49–57.

Qian, H., and E. L. Elson. 1990. Distribution of molecular aggregation by analysis of fluctuation moments. *Proc. Natl. Acad. Sci. USA.* 87: 5479–5483.

Qian, H., and E. L. Elson. 1991. Analysis of confocal laser-microscope optics for 3-D fluorescence correlation spectroscopy. *Appl. Optics.* 30: 1185–95.

Qian, H., E. L. Elson, and C. Frieden. 1992. Studies on the structure of actin gels using time correlation spectroscopy of fluorescent beads. *Biophys. J.* 63:1000–1010.

Rauer, B., E. Neumann, J. Widengren, and R. Rigler. 1996. Fluorescence correlation spectrometry of the interaction kinetics of tetramethylrhodamin α-bungarotoxin with *Torpedo californica* acetylcholine receptor. *Biophys. Chem.* 58:3–12.

Rigler, R., U. Mets, J. Widengren, and P. Kask. 1993. Fluorescence correlation spectroscopy with high count rate and low background: analysis of translational diffusion. *Eur. Biophys. J.* 22:169–175.

Schlessinger, J., D. Axelrod, D. E. Koppel, W. W. Webb, and E. L. Elson. 1977. Lateral transport of a lipid probe and labeled proteins on a cell membrane. *Science.* 195:307–309.

Schneckenburger, H., P. Gessler, and I. Pavenstädt-Grupp. 1992. Measurements of mitochondrial deficiencies in living cells by microspectrofluorometry. *J. Histochem. Cytochem.* 40:1573–1578.

Schwille, P., J. Bieschke, and F. Oehlenschläger. 1997a. Kinetic investigations by fluorescence correlation spectroscopy: the analytical and diagnostic potential of diffusion studies. *Biophys. Chem.* 66:211–228.

Schwille, P., F.-J. Meyer-Almes, and R. Rigler. 1997b. Dual-color fluorescence cross-correlation spectroscopy for multicomponent diffusional analysis in solution. *Biophys. J.* 72:1878–1886.

Southwick, P. L., L. A. Ernst, E. W. Tauriello, S. R. Parker, R. B. Mujumdar, S. R. Mujumdar, H. A. Clever, and A. S. Waggoner. 1990. Cyanine dye labeling reagents—carboxymethylindocyanine succinimidyl esters. *Cytometry.* 11:418–430.

Storrie, B., and T. E. Kreis. 1996. Probing the mobility of membrane proteins inside the cell. *Trends Cell Biol.* 6:321–324.

Terry, B. R., E. K. Matthews, and J. Haselhoff. 1995. Molecular characterization of recombinant green fluorescent protein by fluorescence correlation spectroscopy. *Biochem. Biophys. Res. Commun.* 217:21–27.

Thompson, N. L. 1991. Fluorescence correlation spectroscopy. *In* Topics in Fluorescence Spectroscopy. J. R. Lackowicz, editor. Plenum, New York. 337–377.

Walter, N. G., P. Schwille, and M. Eigen. 1996. Fluorescence correlation analysis of probe diffusion simplifies quantitative pathogen detection by PCR. *Proc. Natl. Acad. Sci. USA.* 93:12805–12810.

Westphal, M., A. Jungbluth, M. Heidecker, B. Mühlbauer, C. Heizer, J.-M. Schwartz, G. Marriott, and G. Gerisch. 1997. Microfilament dynamics during cell movement and chemotaxis monitored using a GFP-actin fusion protein. *Curr. Biol.* 7:176–183.

Widengren, J., Ü. Mets, and R. Rigler. 1995. Fluorescence correlation spectroscopy of triplet states in solution: a theoretical and experimental study. *J. Phys. Chem.* 99:13368–13379.

Widengren, J., and R. Rigler. 1996. Mechanisms of photobleaching investigated by fluorescence correlation spectroscopy. *Bioimaging.* 4:149–157.

Widengren, J., R. Rigler, and Ü. Mets. 1994. Triplet-state monitoring by fluorescence correlation spectroscopy. *J. Fluoresc.* 4:255–258.

Zander, C., M. Sauer, K. H. Drexhage, D.-S. Ko, A. Schulz, J. Wolfrum, L. Brand, C. Eggeling, and C. A. M. Seidel. 1996. Detection and characterization of single molecules in aqueous solution. *Appl. Phys. B.* 63:517–523.